MOLECULAR AND CELLULAR BIOLOGY, July 2008, p. 4494–4506 Vol. 28, No. 14
0270-7306/08/$08.00+0 doi:10.1128/MCB.00074-08

Receptor Type Protein Tyrosine Phosphatase ζ-Pleiotrophin Signaling Controls Endocytic Trafficking of DNER That Regulates Neuritogenesis▽†

Nobuna Fukazawa,[1] Seisuke Yokoyama,[2] Mototsugu Eiraku,[2]‡
Mineko Kengaku,[2] and Nobuaki Maeda[1]*

Department of Developmental Neuroscience, Tokyo Metropolitan Institute for Neuroscience, Tokyo 183-8526, Japan,[1] and Laboratory for Neural Cell Polarity, RIKEN Brain Science Institute, Saitama 351-0198, Japan[2]

Received 15 January 2008/Returned for modification 4 March 2008/Accepted 6 May 2008

Protein tyrosine phosphatase ζ (PTPζ) is a receptor type protein tyrosine phosphatase that uses pleiotrophin as a ligand. Pleiotrophin inactivates the phosphatase activity of PTPζ, resulting in the increase of tyrosine phosphorylation levels of its substrates. We studied the functional interaction between PTPζ and DNER, a Notch-related transmembrane protein highly expressed in cerebellar Purkinje cells. PTPζ and DNER displayed patchy colocalization in the dendrites of Purkinje cells, and immunoprecipitation experiments indicated that these proteins formed complexes. Several tyrosine residues in and adjacent to the tyrosine-based and the second C-terminal sorting motifs of DNER were phosphorylated and were dephosphorylated by PTPζ, and phosphorylation of these tyrosine residues resulted in the accumulation of DNER on the plasma membrane. DNER mutants lacking sorting motifs accumulated on the plasma membrane of Purkinje cells and Neuro-2A cells and induced their process extension. While normal DNER was actively endocytosed and inhibited the retinoic-acid-induced neurite outgrowth of Neuro-2A cells, pleiotrophin stimulation increased the tyrosine phosphorylation level of DNER and suppressed the endocytosis of this protein, which led to the reversal of this inhibition, thus allowing neurite extension. These observations suggest that pleiotrophin-PTPζ signaling controls subcellular localization of DNER and thereby regulates neuritogenesis.

Protein tyrosine phosphatase ζ (PTPζ), also known as RPTPζ/β, is a receptor type protein tyrosine phosphatase that is synthesized as a chondroitin sulfate proteoglycan (12, 16, 17, 21, 28, 32). There are three major splice variants of this molecule, the full-length form (PTPζ-A), the short receptor form (PTPζ-B), and the secreted form (phosphacan) (Fig. 1) (28). PTPζ uses two highly related heparin-binding growth factors, pleiotrophin (PTN) and midkine, as ligands (14, 22–24, 29, 35). PTN has been shown to suppress the tyrosine phosphatase activity of PTPζ by inducing receptor dimerization (10, 29).

PTPζ-PTN signaling has been shown to control neurite extension and cell migration processes probably through the regulation of cytoskeletal dynamics (22, 23, 31, 32). Although several downstream targets of PTPζ such as β-catenin, GIT1/cat-1, and β-adducin have been identified (14, 29, 33), the regulatory mechanism of neuritogenesis by PTPζ-PTN signaling is largely unknown.

We previously demonstrated that PTPζ-PTN signaling is involved in the morphogenesis of cerebellar Purkinje cell dendrites (40, 43). By inhibiting the PTPζ-PTN signaling, aberrant morphogenesis of Purkinje cell dendrites such as multiple and disoriented primary dendrites was induced in a slice culture system (43). In addition, the expression of GLAST, a glial glutamate transporter, in Bergmann glia was also suppressed by the inhibition of PTPζ signaling (43). During development, the dendritic arbors of Purkinje cells elongate in close association with the radial processes of Bergmann glia, and the lamellate processes of Bergmann glia also wrap around the cell bodies and dendrites of Purkinje cells, suggesting that cell-cell interaction between these cells plays important roles in their development (19, 46). Immunohistochemical studies indicated that PTN and phosphacan/PTPζ were deposited in the space between Purkinje cells and the adjacent processes of Bergmann glia, which suggested that PTPζ-PTN signaling mediates the interaction between Purkinje cells and Bergmann glia regulating the differentiation of both types of cells (40).

On the other hand, we recently identified Delta/Notch-like epidermal growth factor (EGF)-related receptor (DNER) (7), a single-pass transmembrane protein with 10 EGF-like repeats in the extracellular domain, which is highly expressed in Purkinje cells (Fig. 1). DNER acts as a ligand of Notch expressed by Bergmann glia and regulates the development of the cerebellar cortex, including the morphogenesis and maturation of Bergmann glia and synapse formation between Purkinje cells and climbing fibers (8, 44). Thus, DNER-Notch signaling plays critical roles in the Purkinje cell-Bergmann glia interaction.

The short cytoplasmic region of DNER contains a tyrosine-based sorting motif, YXXΦ (where X and Φ represent any amino acid and a bulky hydrophobic residue, respectively), and the C-terminal tail with a dileucine motif. The tyrosine-based motif has been shown to be required for dendritic targeting of DNER from the trans-Golgi network and endocytosis of this protein from the plasma membrane (7). In this study, we in-

* Corresponding author. Mailing address: Department of Developmental Neuroscience, Tokyo Metropolitan Institute for Neuroscience, 2-6 Musashidai, Fuchu, Tokyo 183-8526, Japan. Phone: 81-42-325-3881. Fax: 81-42-321-8678. E-mail: maedan@tmin.ac.jp.

† Supplemental material for this article may be found at http://mcb.asm.org/.

‡ Present address: Organogenesis and Neurogenesis Group, RIKEN, Center for Developmental Biology, Kobe 650-0047, Japan.

▽ Published ahead of print on 12 May 2008.

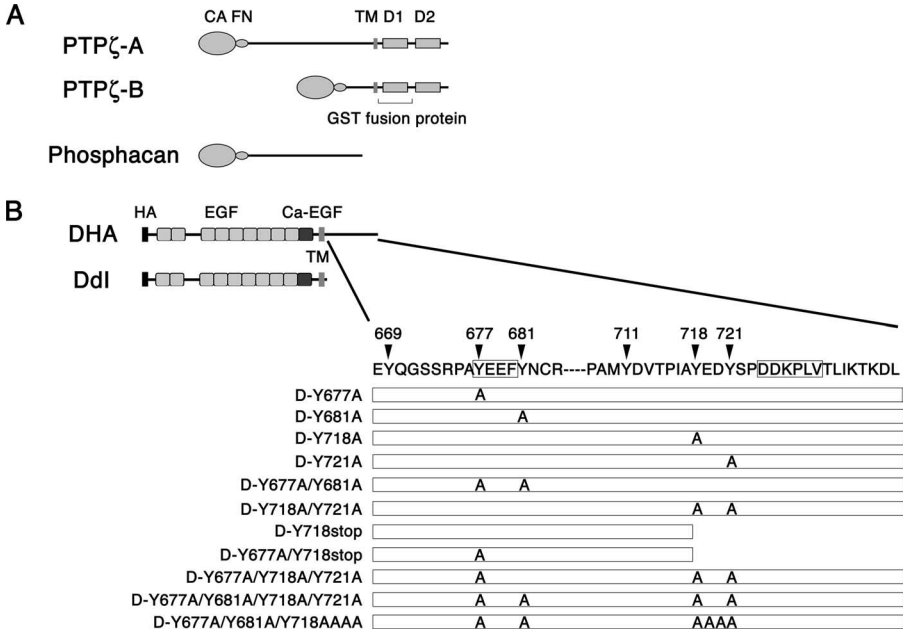

FIG. 1. Schematic representation of PTPζ and DNER. (A) Structures of PTPζ isoforms are schematically shown. CA, carbonic anhydrase-like domain; FN, fibronectin type III domain; TM, transmembrane segment; D1 and D2, tyrosine phosphatase domains. Between the two tyrosine phosphatase domains, only the D1 domain is catalytically active, and the GST fusion protein of this region was used for the in vitro dephosphorylation assay. (B) Schematic representation of DNER and the DNER mutants used for transfection experiments. The residue numbers correspond to those in the amino acid sequence of DNER. DHA is the full-length DNER construct tagged with an HA epitope. D-Y677A, D-Y681A, D-Y718A, and D-Y721A are the full-length DNER mutants that have replacements of the indicated tyrosine residue by alanine. D-Y718stop has a deletion of amino acid residues 718 to 737. D-Y718AAAA has a replacement of amino acid residues 718 to 721 by AAAA. Only the cytoplasmic regions of these mutants are schematically shown. DdI is a DNER mutant lacking the cytoplasmic region. HA, HA epitope tag; EGF, EGF-like domain; Ca-EGF, calcium-binding EGF domain. The tyrosine-based sorting motif and dileucine type sorting motif are boxed.

vestigated the possibility that PTPζ regulates the DNER activity by controlling the tyrosine phosphorylation levels of the DNER cytoplasmic domain. We demonstrate here that the tyrosine residues in and adjacent to the sorting motifs of DNER are phosphorylated, which leads to the accumulation of this protein on the plasma membrane. Accumulation of DNER on the plasma membrane results in the promotion of neurite extension. PTPζ associates with DNER and can dephosphorylate this receptor, raising the possibility that PTPζ-PTN signaling controls the subcellular localization of DNER in neurons and thereby regulates neuritogenesis. Various neurons such as hippocampal and cortical neurons express both DNER and PTPζ (7, 42), raising the possibility that this mechanism regulates neuritogenesis in many brain areas.

MATERIALS AND METHODS

Animals. BALB/c mice were purchased from SLC Inc. (Shizuoka, Japan). All the animal experiments were performed with the approval of the Animal Use and Care Committee of the Tokyo Metropolitan Institute for Neuroscience.

Immunohistochemistry. After ether anesthesia, BALB/c mice were perfused with 4% paraformaldehyde (PFA) in 0.1 M sodium phosphate buffer, pH 7.4. The brains were dissected and postfixed for 4 h in the same solution. The tissues were cryoprotected in 30% sucrose in 0.1 M sodium phosphate buffer, pH 7.4, and frozen with liquid nitrogen. The 30-μm-thick sagittal sections were cut with a cryostat (CM1900; Leica, Houston, TX). The cryosections were treated with 25 mM glycine in phosphate-buffered saline (PBS) for 20 min and washed with 0.3% Triton X-100 in PBS (PBST). The sections were blocked with 5% normal goat serum (NGS) in PBST overnight at 4°C and then incubated with anti-PTPζ (catalog no. 610180; BD Bioscience, San Jose, CA) (1:40) and anti-DNER (7) (1:500) antibodies diluted in 5% NGS-PBST for 3 days at 4°C under free-floating conditions. After being washed with PBST, sections were incubated with Alexa Fluor 488 goat anti-mouse immunoglobulin G (IgG; Invitrogen, Carlsbad, CA) (1:500) and Alexa Fluor 594 goat anti-rabbit IgG (1:500) diluted in 5% NGS-PBS for 2 h. After being washed with PBST, the sections were observed under a confocal laser scanning microscope (FV-1000; Olympus, Tokyo, Japan) using UplanSApo 60× numerical aperture (NA) 1.42 oil and UplanSApo 100× NA 1.40 oil lenses. Results were then processed for publication using Adobe Photoshop 7.0 software (Adobe Systems, Inc., San Jose, CA) with minimal adjustments of brightness and contrast applied to the whole images.

Electron microscopy. BALB/c mice were perfused with 4% PFA containing 0.05% glutaraldehyde in 0.1 M sodium phosphate buffer, pH 7.4. The brains were dissected and postfixed for 4 h in the same solution. The 50-μm-thick sagittal sections were cut on a vibratome (DTK-3000W; Dosaka Co., Kyoto, Japan). The sections were blocked with 4% NGS, 2% bovine serum albumin (BSA), 0.02% Triton X-100 in PBS for 1 h. They were incubated with anti-PTPζ (1:40) or anti-DNER (1:200) antibodies in 1% BSA-PBS for 2 days at 4°C. The sections were incubated with biotinylated anti-mouse IgG (GE Healthcare, Buckinghamshire, England) (1:200) or anti-rabbit IgG (1:200) diluted in PBS for 1 h and then processed using a Vectastain ABC kit (Vector Laboratories, Burlingame, CA). They were then treated with 0.02% 3,3′-diaminobenzidine–0.02% hydrogen peroxide–50 mM Tris-HCl, pH 7.6. The sections were postfixed with 2% OsO_4 in 0.1 M sodium phosphate buffer, pH 7.4, for 45 min; dehydrated using an alcohol series and propylene oxide; and flat embedded in epoxy resin (Quetol 812; Nisshin EM Co., Tokyo, Japan). Ultrathin sections were cut with an ultramicrotome (MT-7000 XL; RMC Products, Tucson, AZ), mounted on Formvar-coated copper grids, and stained with uranyl acetate. Observations were made using a Hitachi H7500 electron microscope (Tokyo, Japan) at 80 kV.

Cell culture, transfection, and immunocytochemistry. Cells were cultured in Dulbecco's modified Eagle's medium (DMEM) (Sigma, St. Louis, MO) supplemented with 10% fetal bovine serum (FBS) (Invitrogen) at 37°C under 5% CO_2. Transfection was performed using Lipofectamine 2000 (Invitrogen) according to the manufacturer's instructions. The coding regions of PTPζ-A and PTPζ-B (32) were ligated into pcDNA3.1 expression vector (Invitrogen). Full-length DNER and the cytoplasmic domain deletion mutant (DdI) cDNAs were hemagglutinin (HA) epitope tagged by being subcloned into the pDisplay expression vector as

previously described (7, 8). Point mutant constructs of DNER were generated by PCR using a full-length construct as template.

Cells were fixed with 4% PFA in PBS for 20 min and permeabilized with 0.1% Triton X-100 in PBS for 10 min. Cells were blocked with 4% NGS–2% BSA-PBS for 30 min and incubated with primary antibodies diluted in 1% BSA-PBS overnight at 4°C. Cells were incubated with Alexa Fluor secondary antibodies diluted in 1% BSA-PBS (1:500) for 30 min. Samples were observed under an FV-1000 confocal laser scanning microscope using a UplanSApo 100× NA 1.40 oil objective lens, and the results were processed as described above.

Immunoprecipitation and immunoblotting. The cerebella were homogenized in 15 volumes of buffer A (0.1 mM phenylmethylsulfonyl fluoride–10 μM pepstatin A–10 μM leupeptin–2 mM sodium vanadate–10 mM sodium fluoride–1 mM sodium pyrophosphate–1 mM EDTA–50 mM Tris-HCl, pH 7.3) containing 0.32 M sucrose. The homogenates were centrifuged at 1,000 × *g* for 5 min at 2°C, and the resultant supernatants (S1 fraction) were used for Western blot analysis using anti-DNER and anti-6B4PG (21) to detect DNER and phosphacan, respectively, as described previously (20, 22). They were also analyzed using anti-actin antibody (A 2066; Sigma). To detect PTPζ and tyrosine-phosphorylated DNER, the S1 fraction was further centrifuged at 100,000 × *g* for 1 h at 2°C, and the resultant precipitates were solubilized with 1% CHAPS {3-[(3-cholamidopropyl)-dimethylammonio]-1-propanesulfonate}-0.15 M NaCl-buffer A. The lysates were subjected to immunoprecipitation using anti-6B4PG and anti-DNER and analyzed by Western blotting using anti-PTPζ or antiphosphotyrosine antibody 4G10 (Upstate Biotechnology, Lake Placid, NY) as described previously (32). Detection of immunoreactive bands was performed using an ECL Plus kit (GE Healthcare).

COS-7 transfectants were solubilized with buffer B (0.15 M NaCl–20 mM HEPES-NaOH, pH 7.4–2 mM $CaCl_2$–2 mM $MgCl_2$–protease inhibitor cocktail [1:50; Nacalai Tesque, Kyoto, Japan]) containing 1% Nonidet P-40 (NP-40), and the solutions were centrifuged at 17,400 × *g* for 10 min at 4°C. The supernatants were incubated with 5 μg/ml of anti-6B4PG or anti-HA polyclonal antibody (Sigma) for 2 h at 4°C and further incubated for 60 min after addition of 25 μl of protein G Sepharose 4FF (GE Healthcare). Normal rabbit IgG (Dako, Carpinteria, CA) was used as control. Immunoprecipitates were washed three times with 0.2% NP-40–buffer B and then washed once with PBS containing 0.9 mM $CaCl_2$ and 0.33 mM $MgCl_2$. The immunoprecipitates were then incubated with 10 mU/ml protease-free chondroitinase ABC (Seikagaku, Tokyo, Japan) in the buffer containing 10 mM Tris-HCl, pH 7.4, 3 mM sodium acetate, 5 mM EDTA, 1 mM phenylmethylsulfonyl fluoride, and 0.1 mM pepstatin A for 15 min at 37°C. The proteins were separated by 5% sodium dodecyl sulfate-polyacrylamide gel electrophoresis (SDS-PAGE) and analyzed by Western blotting with anti-HA monoclonal antibody 12CA5 (Roche, East Sussex, United Kingdom) or anti-6B4PG antibody by using an ECL Plus Western blotting kit.

Cerebella from P7 rats were mixed with 10 volumes of the solution containing 0.32 M sucrose, 2 mM $CaCl_2$, 2 mM $MgCl_2$, 50 mM Tris-HCl, pH 7.3, and protease inhibitor cocktail (1:50) and homogenized in a glass-Teflon Potter homogenizer with 10 strokes at 850 rpm. The homogenates were centrifuged at 1,000 × *g* for 5 min at 4°C, and the resultant supernatants were centrifuged at 100,000 × *g* for 60 min at 4°C. The precipitates were mixed with 1% NP-40–buffer B and gently stirred for 60 min on ice. After centrifugation at 15,000 × *g* for 10 min at 4°C, the supernatants were preadsorbed with protein G Sepharose 4FF by rotating the sample tubes for 2 h at 4°C. After brief centrifugation, the supernatants were subjected to immunoprecipitation using anti-DNER as described above. The immunoprecipitates were analyzed by Western blotting using anti-6B4PG to detect the association of PTPζ/phosphacan and DNER.

In vitro dephosphorylation assay. Glutathione *S*-transferase (GST)-tagged tyrosine phosphatase catalytic domain of rat PTPζ (0.34 U/μg; amino acid residues 1675 to 2021) was expressed in *Escherichia coli* using pGEX-6P-2 vector (GE Healthcare) and purified by using a glutathione-Sepharose 4B column. The phosphatase activities were measured using *p*-nitrophenyl phosphate as described previously (21). One unit is defined as the activity which releases 1 nmol of phosphate per min.

COS-7 cells transfected with DNER constructs were cultured in the presence of 100 μM sodium vanadate for 12 h. The cells were solubilized in buffer C (0.15 M NaCl–20 mM HEPES-NaOH, pH 7.3–5 mM EDTA–2 mM sodium vanadate–5 mM sodium fluoride–10 mM sodium pyrophosphate-protease inhibitor cocktail [1:50]) containing 1% NP-40 and clarified by centrifugation. HA-tagged DNER was immunoprecipitated using anti-HA polyclonal antibody coupled to protein G Sepharose beads, which were washed once with 0.2% NP-40–buffer C and four times with PTP buffer (40 mM imidazole, pH 7.2-0.1 μg/ml BSA-2 mM dithiothreitol). The immunocomplexes were incubated with 0.4 U of GST-tagged tyrosine phosphatase catalytic domain in 25 μl of PTP buffer at 30°C. At the times indicated, the reactions were stopped by adding SDS-PAGE sample buffer, and the samples were boiled for 3 min. Samples were separated by 7.5% SDS-PAGE and analyzed by Western blotting using antiphosphotyrosine antibody 4G10.

Biotinylation of cell surface proteins. The cells were washed with ice-cold PBS twice and incubated with 0.5 mg/ml biotin–X–*N*-hydroxysuccinimide (Calbiochem, La Jolla, CA) dissolved in a borate buffer (10 mM boric acid, 150 mM NaCl, pH 8.0) for 1 h at 4°C. The cells were washed with ice-cold PBS containing 15 mM glycine to terminate biotin coupling and then washed with ice-cold PBS twice. The cells were solubilized in 1% NP-40–buffer C, and the solutions were clarified by centrifugation. The biotinylated proteins were separated using streptavidin agarose (Invitrogen) and analyzed by Western blotting as described above. Quantification by densitometry was done using an Epson GT-9700 scanner (Tokyo, Japan) and Lane Analyzer version 3 software (Atto, Tokyo, Japan).

Organotypic slice culture of cerebellum and biolistic transfection. The methods for slice culture have been described previously (8). In brief, the vermes of the P9 mouse cerebella were cut parasagittally into 370-μm-thick slices in ice-cold Hanks' balanced salt solution containing 20 mM glucose. The slices were mounted on a 3.0-μm porous polycarbonate membrane (Whatman, Maidstone, United Kingdom) that was floated on culture medium in a petri dish. Cerebellar slices were transfected by using a particle-mediated gene transfer device according to the manufacturer's protocols (Helios; Bio-Rad, Hercules, CA) 2 to 5 h after slice preparation. Twenty-five milligrams of 1.0-μm gold particles (Bio-Rad) was coated with 30 μg of pCA-enhanced green fluorescent protein (EGFP) construct (a kind gift from Y. Shima) with or without DdI construct mixed at 1:5. The plasmid-coated particles were delivered with a rapid helium burst of 1.0 MPa to slices that were covered with nylon mesh (70-μm thread spacing; BD Falcon, Bedford, MA) to avoid physical damage. Three days after transfection, cultures were fixed, incubated in 30% sucrose in PBS, and mounted in Crystal/Mount (Biomeda Co., Foster City, CA). The morphology of Purkinje cells visualized by EGFP expression was analyzed with a Zeiss LSM5 Pascal confocal laser scanning microscope using a Plan-Neofluar, 40× NA 1.3 objective lens.

Analysis of the internalization of DNER. Neuro-2A cells transfected with DNER constructs were washed with ice-cold DMEM and then incubated with 10 μg/ml polyclonal rabbit anti-HA antibody in DMEM for 30 min on ice. After being washed with ice-cold DMEM, cells were incubated in DMEM in the presence or absence of 500 ng/ml PTN (R&D Systems, Minneapolis, MN) at 37°C for various periods. Internalization was stopped by adding ice-cold PBS. The cells were fixed with 4% PFA-PBS, permeabilized with 0.1% Triton X-100–PBS, and incubated with Alexa Fluor 488 goat anti-rabbit IgG (1:500). After being washed with PBS, cells were observed under an FV-1000 confocal laser scanning microscope using a UplanSAapo 40× NA 0.90 objective lens. Each experiment was independently repeated three times, and at least 100 cells per experiment were analyzed for each condition. All statistical analyses were performed with the *t* test.

PTN-coated bead assay. Latex beads (particle diameter, 3 μm; Sigma) were coated with 50 μg/ml PTN for 24 h at 4°C and then washed three times with PBS. Neuro-2A cells transfected with DNER constructs were serum starved by culturing them in DMEM containing 0.5% FBS for 18 h and then were stimulated with PTN-coated latex beads for various periods. The cells were solubilized in 1% NP-40–buffer C and subjected to immunoprecipitation as described above. Samples were separated by 7.5% SDS-PAGE and analyzed by Western blotting using anti-HA and antiphosphotyrosine antibody 4G10.

Morphological analysis. Twenty-four-well plates were coated with 50 μg/ml PTN for 24 h at 4°C and then washed three times with PBS. Neuro-2A cells transfected with mock or DNER constructs were seeded at a density of 2×10^4 cells/cm^2 onto PTN-coated 24-well plates and incubated in DMEM containing 5% FBS and 40 μM retinoic acid (Sigma) for 24 h. Transfected cells were identified by immunocytochemistry using anti-HA antibody. Samples were analyzed with a combined differential interference contrast and fluorescence microscope (Axiovert 135; Carl Zeiss, Jena, Germany) using a Plan-Neofluoar 20× NA 0.5 objective lens. Images were acquired with a charge-coupled device camera (Sensyl 1401; Photometrics, Tucson, AZ) operated with MetaMorph software (Molecular Devices, Union City, CA). Neurites were defined as thin protrusions of at least one cell diameter in length. Each experiment was independently repeated three times, and at least 100 cells per experiment were analyzed for each condition. Neurite length was measured by manual tracking of neurites using ImageJ (National Institutes of Health, Bethesda, MD). All statistical analyses were performed using the one-way analysis of variance (ANOVA) and Fisher's protected least significant difference post hoc test built into StatView 5.0 (SAS Institute Inc., Cary, NC).

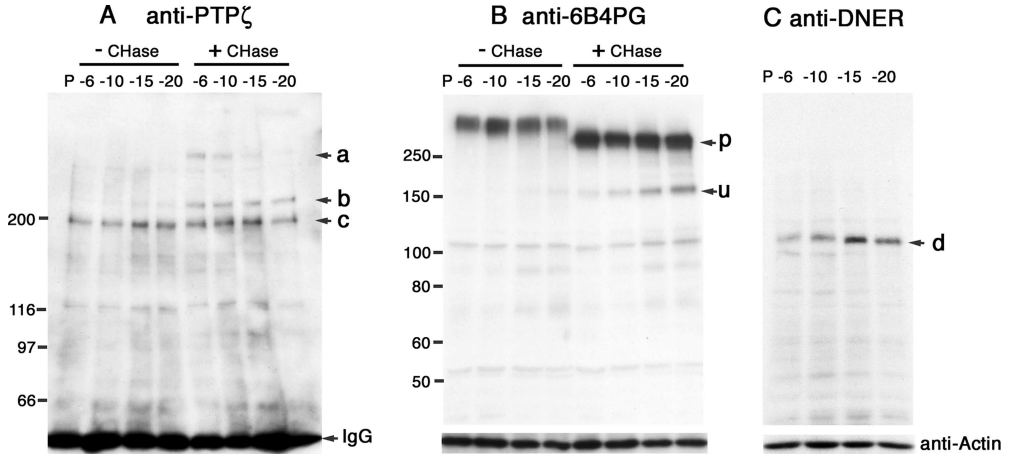

FIG. 2. Expression of PTPζ and DNER in the developing cerebellum. (A) The extracts of P6, P10, P15, and P20 mice cerebella were subjected to immunoprecipitation using anti-6B4PG, and the immunoprecipitates were analyzed by Western blotting with anti-PTPζ before (− CHase) or after (+ CHase) chondroitinase ABC digestion. After chondroitinase ABC digestion, the core proteins of 380-kDa PTPζ-A (a) and 220-kDa PTPζ-B (b) appeared, indicating that both proteins are synthesized as chondroitin sulfate proteoglycans. The 200-kDa bands (c) were constantly detected during postnatal development; they might be a nonglycosylated PTPζ precursor. The bands smaller than 150 kDa are nonspecifically stained ones. (B) The expression of phosphacan was examined by Western blotting using anti-6B4PG before or after chondroitinase ABC digestion. The 300-kDa core protein of phosphacan (p) was constantly detected during postnatal development. A minor 150-kDa band was also detected after chondroitinase ABC digestion (u); it might be a degradation product. Numbers at left of panels A and B are molecular masses in kilodaltons. (C) The expression of DNER was examined by Western blotting using anti-DNER. The expression of DNER increased from P6 to P15 and decreased thereafter (d). As a loading control, the blots were reprobed with antiactin antibody.

RESULTS

Developmental expression of PTPζ and DNER in the cerebellum. To examine the developmental expression of PTPζ and DNER, we performed immunoblot analysis using mouse cerebella. Before chondroitinase ABC digestion, PTPζ-A and -B were detected as smears on the immunoblots by using monoclonal antibody against the intracellular domain of PTPζ, anti-PTPζ (Fig. 2A, left). After chondroitinase ABC digestion, however, sharp 380- and 220-kDa bands were detected (Fig. 2A, a and b), which correspond to PTPζ-A and PTPζ-B, respectively (32), indicating that both molecules were expressed as chondroitin sulfate proteoglycans. Comparable amounts of PTPζ-A and PTPζ-B were detected at postnatal day 6 (P6), and thereafter, the expression of PTPζ-A was downregulated (Fig. 2A). On the other hand, PTPζ-B was constantly expressed during postnatal cerebellar development (Fig. 2A). In addition to these isoforms, a 200-kDa band was detected at each developmental stage (Fig. 2A, c). The electrophoretic mobility of this band was not changed after chondroitinase ABC digestion, indicating that it is not a proteoglycan. This might be a nonglycosylated precursor of PTPζ, although further studies are necessary to reveal this point.

Immunoblotting using antibodies against the extracellular domain of PTPζ (anti-6B4PG) indicated that phosphacan was abundantly expressed during postnatal development (Fig. 2B).

DNER showed dynamic changes of expression during cerebellar development. Its expression was upregulated from P6 to P15 and downregulated thereafter (Fig. 2C). From this finding, we hypothesized that DNER is involved in the dendrite formation of Purkinje cells, which occurs vigorously from P6 to P15 (40).

Immunohistochemical localization of PTPζ and DNER in the cerebellum. We next examined the immunohistochemical localization of PTPζ and DNER by double labeling using anti-DNER and anti-PTPζ. In the P21 mouse cerebellum, the cell bodies and dendrites of Purkinje cells were clearly stained by anti-DNER (Fig. 3B). On the other hand, the PTPζ immunoreactivity was broadly observed in the cerebellar cortex, including the molecular layer, Purkinje cell layer, and granule cell layer (Fig. 3A). In the molecular layer, the Purkinje cell dendrites were relatively intensely stained by anti-PTPζ (Fig. 3A). As revealed by higher-magnification images, both PTPζ and DNER immunoreactivities showed patchy distribution in the dendritic shafts of Purkinje cells (Fig. 3D and E). Merged images revealed that a part of these patches were stained by both the antibodies (Fig. 3F). It is noteworthy that there was almost no overlapping distribution outside of the thick dendritic shafts of Purkinje cells.

Immunoelectron microscopy indicated that the immunoreactivity to anti-PTPζ was localized on the cell surfaces of Purkinje cells as patchy stainings and on cytoplasmic vesicles (Fig. 3G and I). The staining with anti-PTPζ was frequently detected on the Purkinje cell surface contacting Bergmann glial processes (Fig. 3G, arrowheads). The cell surfaces of Bergmann glial processes were also stained by anti-PTPζ (Fig. 3J), consistent with the in situ hybridization experiments indicating that both Purkinje cells and Bergmann glia express PTPζ (42). The immunoreactivity to anti-DNER was distributed on the plasma membrane of Purkinje cells but not in the Bergmann glial processes (Fig. 3K). The staining showed patchy distribution and was often observed on the Purkinje cell surface contacting the Bergmann glial processes. In addition, vesicles of various sizes in the Purkinje cell dendrites were stained with anti-DNER (Fig. 3L). These observations suggest that the patchy colocalization of PTPζ and DNER immunoreactivities in immunofluorescent microscopy corresponded to the vesicles and/or plasma membrane of Purkinje cells.

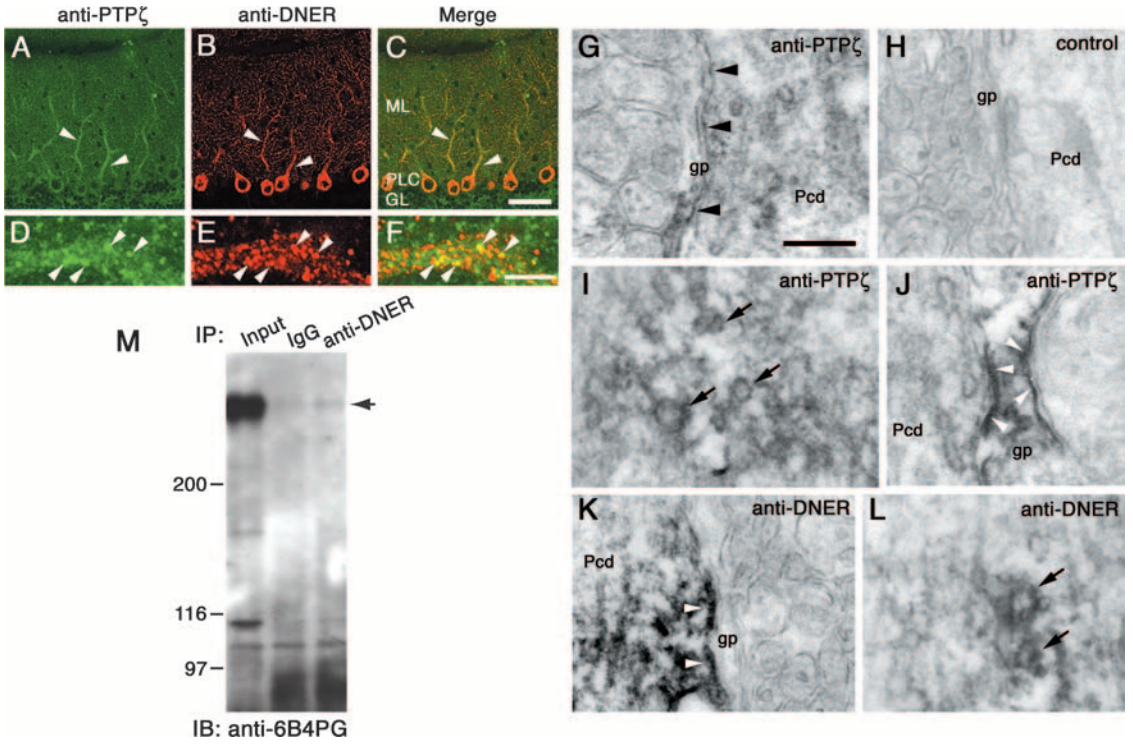

FIG. 3. Immunohistochemical localization and association of PTPζ and DNER in the cerebellar cortex. Sagittal sections from P21 mouse cerebella were double immunostained with anti-PTPζ (A and D, green) and anti-DNER (B and E, red). Panels C and F are merged images. PTPζ immunoreactivity was detected broadly in the cerebellar cortex, but the thick dendritic shafts of the Purkinje cells were relatively intensely stained (A, arrowheads). DNER immunoreactivity was observed specifically in the Purkinje cell dendrites and cell bodies (B). Higher-magnification images revealed that both immunoreactivities showed patchy colocalization in the dendritic shafts of Purkinje cells (F, arrowheads). ML, molecular layer; PLC, Purkinje cell layer; GL, granule cell layer. Bars, 50 μm (C) and 5 μm (F). Sagittal sections from P21 mouse cerebella were stained with anti-PTPζ (G, I, and J) or anti-DNER (K and L) and were observed under an electron microscope. (H) Negative-control section. Cell surface of Purkinje cell dendrites (G, arrowheads) and Bergmann glia (J, arrowheads) showed PTPζ immunoreactivities. A portion of the vesicles in the Purkinje cell dendrites also showed PTPζ immunoreactivity (I, arrows). DNER immunoreactivity was observed on the Purkinje cell surface (K, arrowheads) and on a portion of cytoplasmic vesicles (L, arrows). Pcd, Purkinje cell dendrites; gp, Bergmann glial processes. Bar, 250 nm. (M) Lysates of P7 rat cerebella were subjected to immunoprecipitation using anti-DNER and control IgG. The immunoprecipitates were analyzed by Western blotting using anti-6B4PG. PTPζ/phosphacan was coimmunoprecipitated with DNER. The intense band detected in the left lane (Input) corresponds to phosphacan. Numbers at left are molecular masses in kilodaltons.

Interaction of PTPζ and DNER. We next examined whether PTPζ interacts with DNER by immunoprecipitation experiments. Lysates of P7 rat cerebella were subjected to immunoprecipitation experiments using anti-DNER or control rabbit IgG, and the precipitated proteins were analyzed by immunoblotting with anti-6B4PG. After chondroitinase ABC digestion, a faint but significant 300- to 400-kDa band was detected by Western blot analysis of the immunoprecipitates (Fig. 3M). We could not determine whether this band corresponds to phosphacan or to PTPζ-A because of the low titer of anti-PTPζ.

We further investigated the association of PTPζ and DNER by cotransfection experiments using COS-7 cells. Confocal microscopic analysis of the COS-7 cells transiently expressing PTPζ-A and DNER tagged with an HA epitope (DHA [Fig. 1]) indicated that both proteins were partially colocalized in the intracellular granular compartments, especially around nuclei (Fig. 4A to D). While PTPζ-A was detected both on the cell surface and in the intracellular granules, most of the DNER signals showed a punctate pattern at the perinuclear cytoplasm. The COS-7 cells coexpressing PTPζ-B and DNER showed similar staining patterns (Fig. 4E to H). In sharp contrast, when a DNER construct lacking most of the intracellular domain (DdI [Fig. 1]) was coexpressed with PTPζ-A, signals of both proteins were clearly colocalized at the cell surface (Fig. 4I to L) (see Fig. S1 in the supplemental material for quantitative evaluation). We found little intracellular punctate signal. Cotransfectants expressing PTPζ-B and DdI showed similar cell surface staining (Fig. 4M to P).

In spite of such distinct subcellular localizations, PTPζ was coimmunoprecipitated with both DHA and DdI (Fig. 5), suggesting that the interaction is mediated by the extracellular and/or transmembrane regions of DNER. In order to examine the possibility of *trans* interaction, we incubated the DdI transfectants in solutions containing phosphacan (up to 0.2 μM) and then stained the cells with anti-6B4PG. However, we observed no significant binding of phosphacan to the cells expressing DdI on the plasma membrane (data not shown). These observations suggest that PTPζ and DNER interact in a *cis* manner and that their subcellular localization is regulated by the cytoplasmic region of DNER.

Tyrosine phosphorylation of DNER. The cytoplasmic region of DNER contains a tyrosine-based sorting motif (YXXΦ),

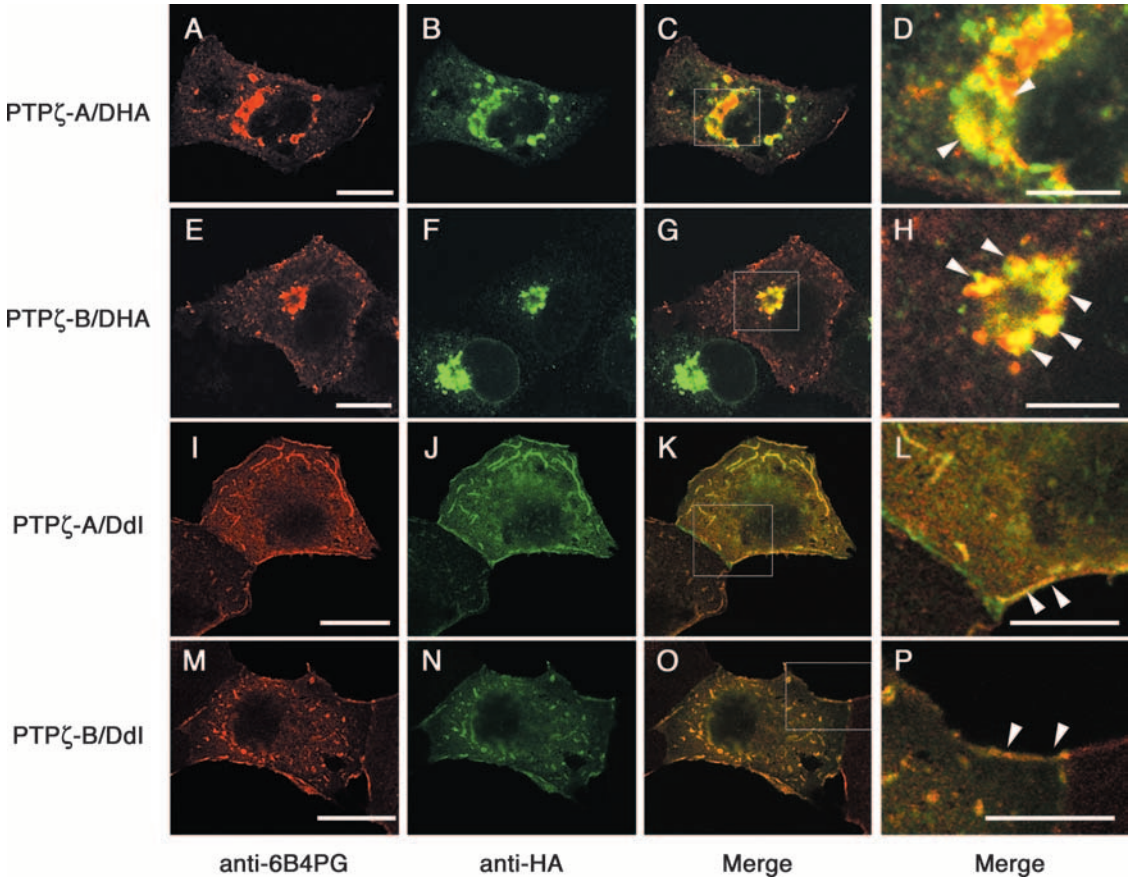

FIG. 4. Colocalization of PTPζ and DNER in COS-7 transfectants. COS-7 cells were cotransfected with PTPζ-A and DHA (A to D), PTPζ-B and DHA (E to H), PTPζ-A and DdI (I to L), or PTPζ-B and DdI (M to P) constructs. The cells were doubly stained with anti-6B4PG (A, E, I, and M; red) and anti-HA (B, F, J, and N; green) antibodies. The merged images are shown in panels C, G, K, and O. Higher-magnification images of the areas enclosed by rectangles in panels C, G, K, and O are shown in panels D, H, L, and P, respectively. Both PTPζ-A and -B showed colocalization with DHA in the cytoplasmic granules (D and H, arrowheads). On the other hand, DdI showed colocalization with PTPζ-A and -B at the plasma membrane (L and P, arrowheads). Bars, 20 μm (A, E, I, and M) and 10 μm (D, H, L, and P).

which is involved in dendritic targeting of DNER. DNER also contains a C-terminal dileucine type motif, which has been shown to play important roles in polarized targeting and endocytosis of transmembrane proteins (6). Furthermore, the DNER cytoplasmic region contains several tyrosine residues potentially phosphorylated by tyrosine kinases, including the YXXΦ motif.

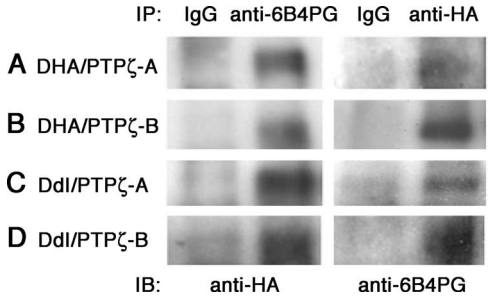

FIG. 5. Association of PTPζ and DNER in COS-7 transfectants. Cell lysates of the COS-7 cotransfectants expressing DHA and PTPζ-A (A), DHA and PTPζ-B (B), DdI and PTPζ-A (C), and DdI and PTPζ-B (D) were subjected to immunoprecipitation using anti-6B4PG, anti-HA, or control IgG. The immunoprecipitates were analyzed by Western blotting using anti-HA or anti-6B4PG.

Immunoblot analysis of DNER immunoprecipitated from P15 mouse cerebella indicated that this protein was weakly tyrosine phosphorylated in vivo (Fig. 6A). We next treated the COS-7 transfectants expressing DHA with sodium vanadate, a tyrosine phosphatase inhibitor. The immunoprecipitated DHA from these cells was tyrosine phosphorylated, as revealed by immunoblot analysis using antiphosphotyrosine antibody (Fig. 6B). We further examined whether DNER can serve as a substrate for PTPζ. COS-7 transfectants expressing DHA were treated with sodium vanadate, and then the DHA was immunoprecipitated with anti-HA antibody. When the immunoprecipitated tyrosine-phosphorylated DHA was treated with the catalytic domain of PTPζ, DHA was dephosphorylated (Fig. 6C).

We noticed that there are four potential tyrosine phosphorylation sites in the cytoplasmic region of DNER: Tyr-677, Tyr-681, Tyr-718, and Tyr-721. Among these sites, Tyr-677 is a part of the tyrosine-based sorting motif, YEEΦ (Fig. 1B). The positions of Tyr-718 and -721 are close to the second C-terminal sorting motif (Fig. 1B). To investigate which tyrosine residues are phosphorylated, we prepared various DNER constructs, in which several of

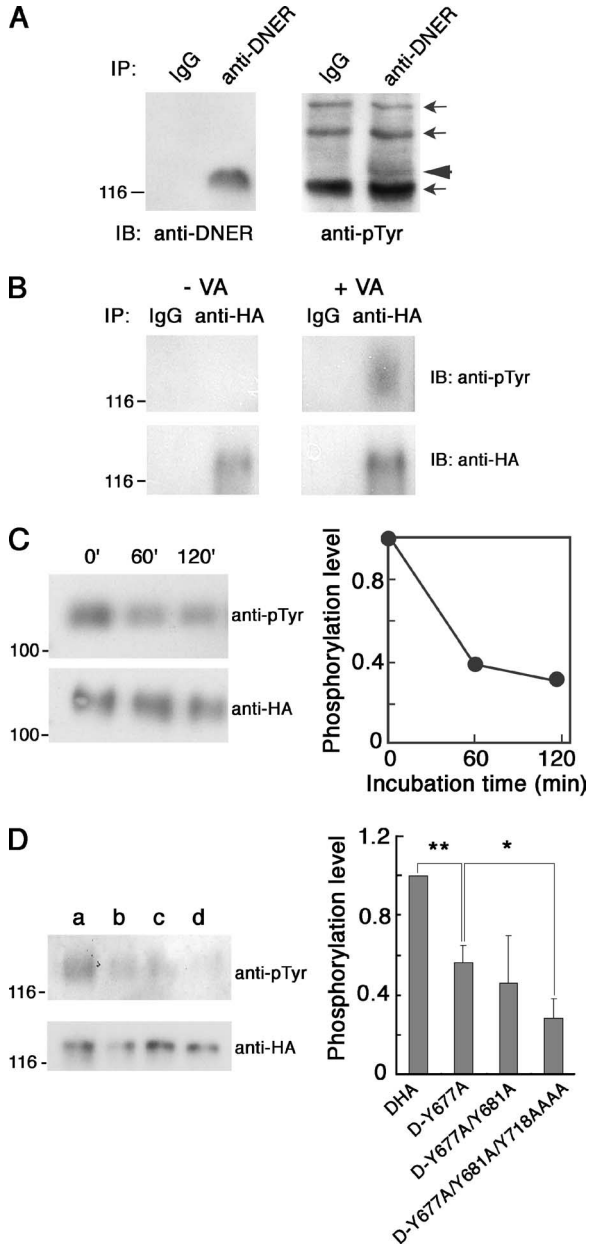

FIG. 6. Tyrosine phosphorylation of DNER in vivo and in vitro. (A) Lysates of the P15 mouse cerebella were subjected to immunoprecipitation using anti-DNER or control IgG. The precipitated proteins were analyzed by Western blotting using anti-DNER or antiphosphotyrosine antibodies (anti-pTyr). The arrowhead indicates the band of tyrosine-phosphorylated DNER. Several bands were nonspecifically precipitated and stained by antiphosphotyrosine antibody (arrows). (B) COS-7 transfectants expressing DHA were treated with 100 μM sodium vanadate (VA) for 6 h, and then the cell lysates were subjected to immunoprecipitation using anti-HA or control IgG. The immunoprecipitates were analyzed by Western blotting with anti-HA or antiphosphotyrosine antibodies. The tyrosine-phosphorylated DNER was often detected as a broad band larger than the band of nonphosphorylated DNER, probably because there were differentially phosphorylated DNER proteins. (C) COS-7 transfectants expressing DHA were treated with 100 μM sodium vanadate for 12 h, and the cell lysates were subjected to immunoprecipitation using anti-HA antibodies. The immunoprecipitates were treated with 0.4 U of GST-tagged catalytic domain of PTPζ for various periods. Then the samples were analyzed by Western blotting with antiphosphotyrosine or anti-HA antibodies (left). The tyrosine phosphorylation levels of DNER were quantified by densitometry (right). (D) COS-7 transfectants expressing DHA (a), D-Y677A (b), D-Y677A/Y681A (c), or D-Y677A/Y681A/Y718AAAA (d) were treated with 100 μM sodium vanadate for 12 h, and the cell lysates were subjected to immunoprecipitation using anti-HA antibodies. The immunoprecipitates were analyzed by Western blotting with antiphosphotyrosine and anti-HA antibodies (left). The tyrosine phosphorylation levels of DNER mutants were quantified by densitometry (right). Data are means ± standard deviations of four determinations. Asterisks indicate statistical significance (*, $P < 0.05$; **, $P < 0.001$; one-way ANOVA). Numbers at left of panels indicate molecular masses in kilodaltons.

these tyrosine residues were replaced with alanine (Fig. 1B). COS-7 cells transfected with these DNER constructs were treated with sodium vanadate, and then the tyrosine phosphorylation levels of these mutants were analyzed by immunoblotting (Fig. 6D). D-Y677A showed a significantly decreased tyrosine phosphorylation level compared with that of the control, DHA, indicating that the tyrosine-based sorting motif itself could be phosphorylated (Fig. 6D). D-Y677A/Y681A/Y718AAAA showed a further-reduced tyrosine phosphorylation level compared with those of D-Y677A and D-Y677A/Y681A, suggesting that Tyr-718 and/or Tyr-721 could also be phosphorylated (Fig. 6D).

Subcellular localization of DNER regulated by tyrosine phosphorylation. Since it became apparent that an important sorting motif in the cytoplasmic region of DNER is tyrosine phosphorylated, we next investigated whether the subcellular localization of DNER is regulated by tyrosine phosphorylation. As described above, most DHA protein showed intracellular distribution in the COS-7 cells coexpressing DHA and PTPζ-B (Fig. 7A, a to c). In contrast, DHA protein accumulated on the cell surface and was colocalized with PTPζ-B after sodium vanadate treatment (Fig. 7A, d to f) (see Fig. S2 in the supplemental material for a Z-stack image). We next evaluated the presence of DHA protein on the plasma membrane after sodium vanadate treatment by cell surface biotinylation experiments. Western blot analysis clearly indicated that biotinylated cell surface DHA protein was remarkably increased by sodium vanadate in the cells coexpressing DHA and PTPζ (Fig. 7B and C).

Regulation of the subcellular localization of DNER by the sorting motifs. To examine which sites are required for the regulation of the subcellular localization of DNER, we transfected Neuro-2A neuroblastoma cells with various DNER constructs listed in Fig. 1. As in the case of COS-7 transfectants, the full-length form of DNER (DHA) showed perinuclear cytoplasmic localization (Fig. 8A), and DdI exhibited cell surface distribution (Fig. 8E). While most of the mock-transfected and DHA-expressing Neuro-2A cells showed a rounded cell shape, a substantial portion (20 to 30%) of the DdI-expressing cells displayed thick cell processes, suggesting that the cell surface expression of DNER is involved in the regulation of the morphogenesis of neurons (Fig. 8E).

When Neuro-2A cells were transfected with the D-Y677A or D-Y681A constructs, in which the tyrosine-based motif is destroyed, these DNER mutants showed normal perinuclear cytoplasmic localization, like that of DHA (Fig. 8F). D-Y718A, D-Y721A, and D-Y718A/Y721A also showed normal subcellular

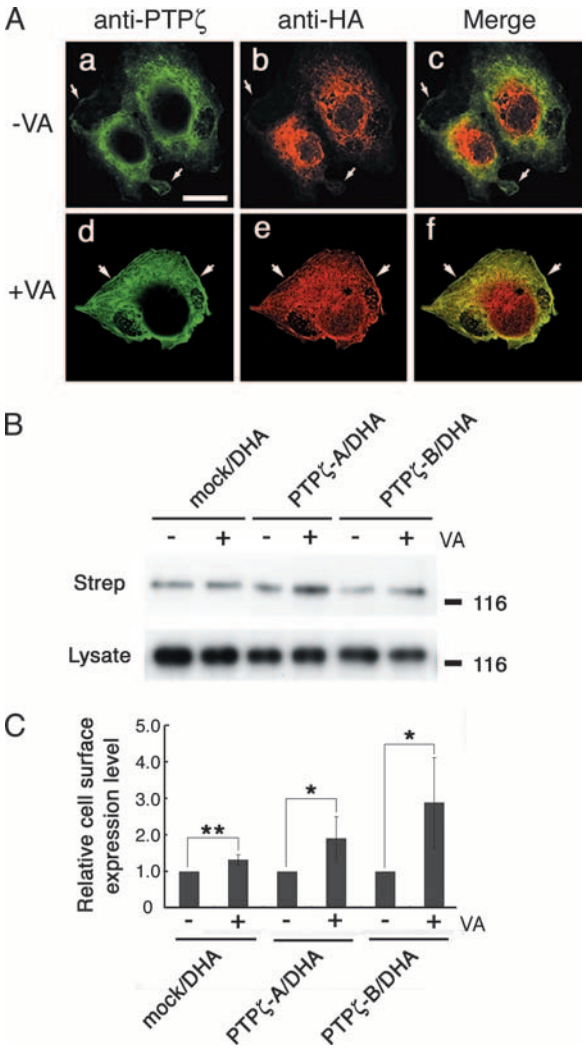

FIG. 7. Regulation of the subcellular localization of DNER by tyrosine phosphorylation. (A) COS-7 transfectants expressing both DHA and PTPζ-B were cultured in the presence (d to f) or absence (a to c) of 100 μM sodium vanadate (VA) for 12 h. The cells were permeabilized and stained with anti-HA (b and e; red) and anti-PTPζ (a and d; green), which recognizes the D2 domain of PTPζ. The merged images are shown in subpanels c and f. In the presence of sodium vanadate, PTPζ-B and DHA showed colocalization on the cell surface (f). In the absence of sodium vanadate, PTPζ immunoreactivity was detected on the cell surface and in the cytoplasm (a), and DNER immunoreactivity was accumulated around the nucleus (b). In this case, the colocalization of the two immunoreactivities around the nucleus was not remarkable in contrast to the results shown in Fig. 4. In Fig. 4, the cells were doubly stained with anti-HA and anti-6B4PG, which recognizes the extracellular region of PTPζ. This suggests that the D2 domain of PTPζ is proteolytically processed or modified during intracellular trafficking. The cell peripheries are indicated by arrows. Bar, 20 μm. (B) COS-7 transfectants expressing DHA and PTPζ were cultured in the presence or absence of 100 μM sodium vanadate for 12 h, and cell surface proteins were biotinylated at 4°C. The biotinylated proteins were separated with streptavidin agarose and analyzed by Western blotting using monoclonal anti-HA antibody to detect cell surface DHA (Strep). The expression levels of DHA were examined by Western blot analysis of the cell lysates using anti-HA (Lysate). Treatment with sodium vanadate increased the cell surface expression of DHA. Numbers at right are molecular masses in kilodaltons. (C) Cell surface expression levels of DHA were quantified by densitometric analysis of the Western blots shown in panel B. Data are means ± standard deviations of four determinations. Asterisks indicate statistical significance (*, $P < 0.05$; **, $P < 0.01$; t test).

localization (Fig. 8F). In contrast, D-Y718stop, which lacks the C-terminal 20 amino acids, showed increased cell surface expression (3.9% ± 1.9% for DHA versus 41.6% ± 21.5% for D-Y718stop) (Fig. 8B, C, and F), suggesting that the C-terminal portion plays major roles in the internalization of DNER in this expression system. However, the function of the tyrosine-based motif became apparent when a mutation of this motif was introduced into the D-Y718stop construct. In contrast to the D-Y677A and D-Y718stop mutants, the D-Y677A/Y718stop mutant displayed almost complete cell surface localization (88.5% ± 5.7% for D-Y677A/Y718stop) (Fig. 8F). Moreover, the D-Y677A/Y718A/Y721A and D-Y677A/Y681A/Y718A/Y721A mutants showed fairly increased cell surface expression compared with DHA and the D-Y718A/Y721A mutant (Fig. 8F), consistent with the observation that sodium vanadate treatments increased the cell surface expression of DHA (Fig. 7). Like DdI-expressing cells, the Neuro-2A cells expressing D-Y677A/Y718stop often showed thick processes (Fig. 8D). These observations indicated that the tyrosine residues in the cytoplasmic domain of DNER play important roles in the determination of the subcellular localization of this protein.

Next, we transfected the DdI construct into Purkinje cells by using an organotypic slice culture system of cerebellum (Fig. 8G to L). While most Purkinje cells had a single primary dendrite in the control culture (Fig. 8G and H), most DdI-expressing Purkinje cells had two or more primary dendrites (Fig. 8I and J). This phenotype is very similar to that observed when PTPζ-PTN signaling was inhibited (43), suggesting that this signaling system regulates the subcellular localization of DNER.

PTN regulates the endocytosis of DNER in Neuro-2A cells. DNER is actively endocytosed from the plasma membrane and delivered to the EEA1-positive early endosomes, and this sorting is thought to be mediated by the tyrosine-based signal in DNER (7). The above experiments indicated that a tyrosine residue in this sorting signal is phosphorylated (Fig. 6) and that the inhibition of tyrosine phosphatase activities by sodium vanadate inhibited the endocytosis of DNER in the COS-7 cells coexpressing DNER and PTPζ (Fig. 7). On the other hand, the tyrosine phosphatase activity of PTPζ is inactivated by PTN stimulation through receptor dimerization (10, 29). Therefore, we hypothesized that PTN-PTPζ signaling regulates the endocytosis of DNER by controlling the tyrosine phosphorylation levels of this protein. To test this possibility, we performed experiments using Neuro-2A cells, which express endogenous PTPζ-A and -B but not DNER, as revealed by reverse transcription-PCR analysis (data not shown). The Neuro-2A cells were transfected with DHA or D-Y718stop constructs, and the cell surface-expressed proteins were labeled with anti-HA antibody. The cells were incubated for various times in the presence or absence of PTN, and the DNER proteins that were internalized or remained on the cell surface were visualized using fluorescently labeled secondary antibodies. We classified the DNER localization into three types: type I, intracellular localization; type II, cell surface and intracellular localization; and type III, cell surface localization (Fig. 9B).

In the control culture, antibody-labeled DHA proteins were rapidly internalized, and internalization of DHA was only slightly delayed even in the presence of PTN (Fig. 9A, a, c, and e). The time required for 50% of the cells to show type I

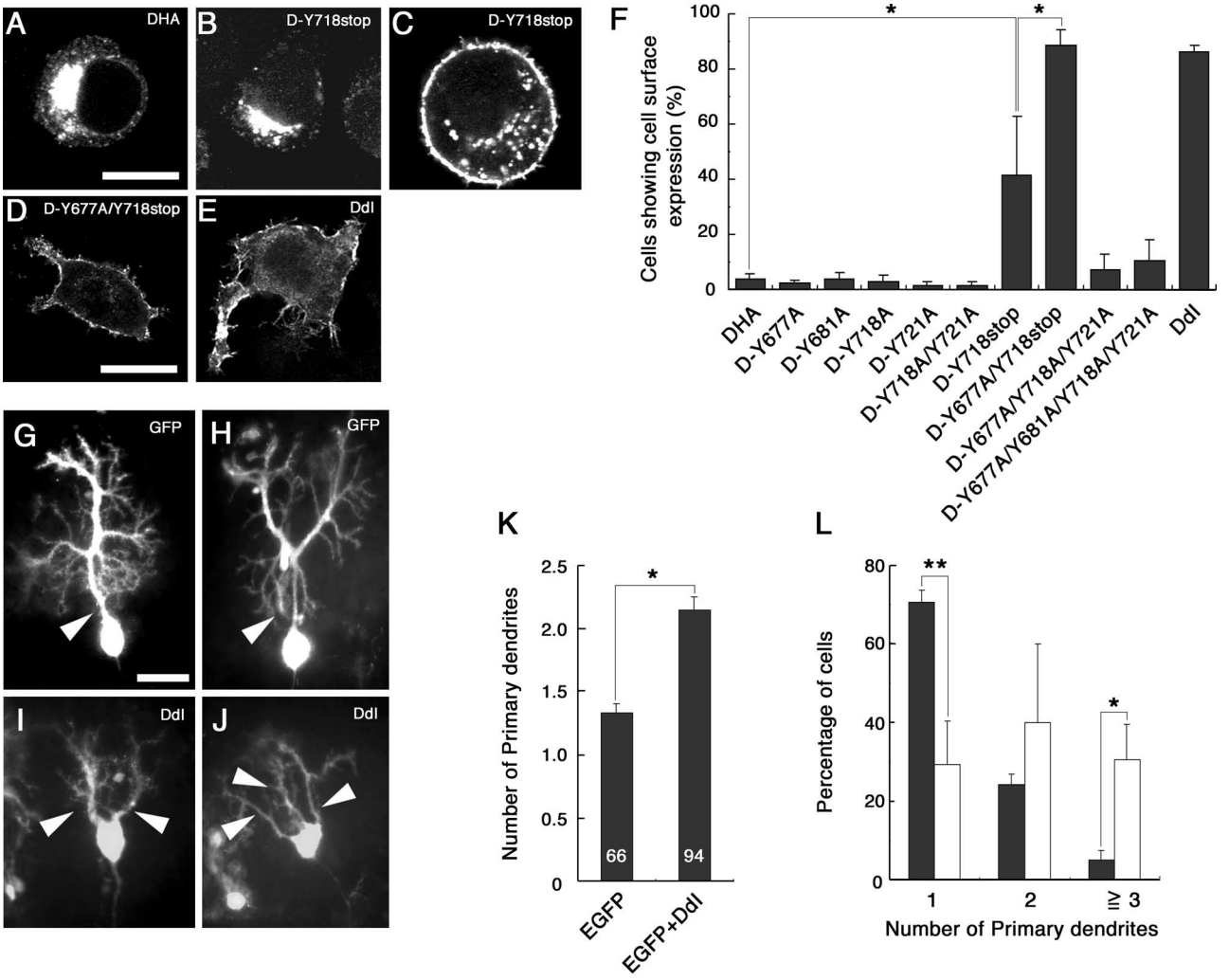

FIG. 8. Subcellular localization of DNER mutants and morphological changes of cells induced by cell surface expression of them. Neuro-2A cells were transfected with DHA (A), D-Y718stop (B and C), D-Y677A/Y718stop (D), or DdI (E) constructs and were immunostained with anti-HA antibody. Most of the Neuro-2A cells expressing DHA showed intracellular perinuclear staining (A). The D-Y718stop-expressing cells showed intracellular (B) and cell surface (C) staining. Most D-Y677A/Y718stop (D)- and DdI (E)-expressing cells showed cell surface staining, in which ~30% of the cells extended several protrusions. Bars, 20 μm (A to C) and 10 μm (D and E). (F) The percentages of the cells that showed cell surface staining were summarized for Neuro-2A transfectants expressing DHA, D-Y677A, D-Y681A, D-Y718A, D-Y721A, D-Y718A/Y721A, D-Y718stop, D-Y677A/Y718stop, D-Y677A/Y718A/Y721A, D-Y677A/Y681A/Y718A/Y721A, and DdI. Data are means ± standard deviations of triplicate determinations. Asterisks indicate statistical significance (*, $P < 0.0001$, one-way ANOVA). Purkinje cells were transfected with EGFP (G and H) or EGFP plus DdI (I and J) constructs in cerebellar slice cultures. While control Purkinje cells possessed a single primary dendrite (G and H, arrowhead), most DdI-expressing Purkinje cells showed multiple primary dendrites (I and J, arrowheads). Bar, 25 μm (G to J). The mean number of primary dendrites (K) and the distribution of the number of primary dendrites of control (solid columns) and DdI-expressing cells (open columns) (L) were quantified. Data are means ± standard deviations of triplicate experiments in panels K and L. Asterisks indicate statistical significance (*, $P < 0.001$, t test in panel K; *, $P < 0.05$, and **, $P < 0.0001$, one-way ANOVA in panel L).

localization ($T_{1/2}$) was 2.9 ± 0.6 min for the control culture. In the presence of PTN, $T_{1/2}$ was 4.7 ± 0.5 min ($P < 0.05$ versus control; t test). The data in Fig. 8 indicated that the C-terminal portion plays a major role in the endocytosis of DNER in Neuro-2A cells. Although Tyr-718 and/or Tyr-721 could be tyrosine phosphorylated (Fig. 1 and Fig. 6), their phosphorylation might not interfere with the function of the C-terminal motif. On the other hand, the tyrosine-based sorting motif could be directly phosphorylated, and therefore, its function is expected to be regulated by phosphorylation. Thus, we next analyzed Neuro-2A cells expressing the D-Y718stop mutant which has only the tyrosine-based sorting motif (Fig. 1). D-Y718stop mutant proteins took a longer time ($T_{1/2}$ = 7.3 ± 0.5 min) to be internalized than did DHA (Fig. 9A, b, d, and f). In addition, PTN significantly decreased the rate of internalization of D-Y718stop proteins ($T_{1/2}$ = 11.0 ± 0.5 min) ($P <$ 0.01 versus control; t test) (Fig. 9A, b and d), suggesting that PTN suppressed the function of the tyrosine-based sorting motif by inducing the tyrosine phosphorylation of this motif.

In order to confirm that PTN stimulates the tyrosine phosphorylation of DNER, Neuro-2A cells expressing DHA were treated with PTN-coated beads for various periods (Fig. 9C).

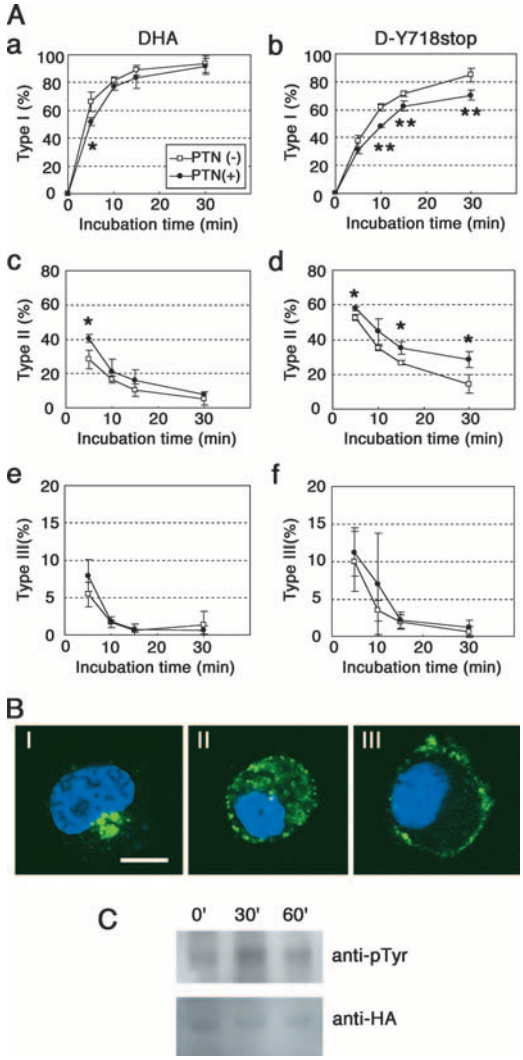

FIG. 9. Suppression of the internalization of DNER by PTN in Neuro-2A cells. (A) Neuro-2A transfectants expressing DHA (a, c, and e) or D-Y718stop (b, d, and f) were treated with anti-HA antibody on ice for 30 min and then incubated in the presence (solid circles) or absence (open squares) of 0.5 μg/ml PTN at 37°C for various periods. The localization of DNER labeled with anti-HA antibody was visualized with Alexa Fluor 488 goat anti-rabbit IgG after permeabilization. Subcellular localization of DNER was classified into three types: type I, intracellular localization; type II, cell surface and intracellular localization; and type III, cell surface localization. The percentages of the cells that showed type I (a and b), type II (c and d), and type III (e and f) localization at each time point were evaluated. Data are means ± standard deviations of triplicate determinations. Asterisks indicate statistical significance (*, $P < 0.05$; **, $P < 0.01$, *t* test). (B) Three types of cells showing different localization of DHA (green). The staining with Hoechst 33258 is shown in blue. Bar, 10 μm. (C) Neuro-2A transfectants expressing DHA were stimulated with PTN-coated latex beads for 0, 30, and 60 min. The cell lysates were subjected to immunoprecipitation using anti-HA, and then the immunoprecipitates were analyzed by Western blotting with anti-HA or antiphosphotyrosine (anti-pTyr) antibodies.

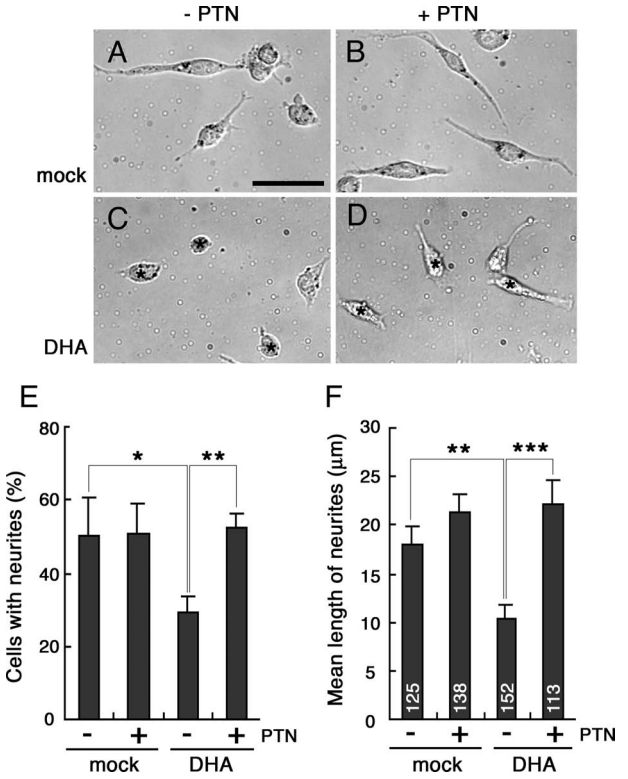

FIG. 10. Inhibition of DNER activity by PTN in the retinoic-acid-induced neurite outgrowth of Neuro-2A cells. Neuro-2A cells transfected with mock (A and B) or DHA (C and D) constructs were cultured in the presence of 40 μM retinoic acid for 24 h on culture plates coated (B and D) or not coated (A and C) with 50 μg/ml PTN. Bar, 50 μm (A to D). The percentages of neurite-bearing cells (E) and the mean lengths of neurites per cell (F) were measured. Data are means ± standard deviations of triplicate determinations in panel E and means ± standard errors of the means in panel F. Asterisks indicate statistical significance (*, $P < 0.05$; **, $P < 0.01$; ***, $P < 0.0001$; one-way ANOVA) in panels E and F.

PTN stimulation transiently increased the tyrosine phosphorylation level of DHA. In this experiment, the effects of PTN-coated beads instead of the soluble form were examined because the effects of soluble PTN were low and it was hard to detect the changes in tyrosine phosphorylation levels of PTPζ substrates (14).

Effects of PTN on the DNER-dependent inhibition of neuritogenesis of Neuro-2A cells. The Neuro-2A cells overexpressing DdI or D-Y677A/Y718stop mutants displayed expanded morphology and extended many protrusions (Fig. 8). These mutant DNER proteins were accumulated on the cell surface, and their endocytosis was suppressed, suggesting that blockage of DNER endocytosis leads to morphological changes of cells, possibly including neuritogenesis. Thus, next we examined the effects of PTN on the neuritogenesis of Neuro-2A cells expressing DHA because PTN suppressed the endocytosis of this protein (Fig. 9).

Neuro-2A cells differentiate and extend neurites in response to retinoic acid (30). As described above, Neuro-2A cells expressed PTPζ but not DNER. Western blotting indicated that the treatment of Neuro-2A cells with 40 μM retinoic acid for 24 h did not alter the expression levels of these proteins (data not shown). We first cultured Neuro-2A cells on PTN-coated plates in the presence of retinoic acid (Fig. 10). Instead of adding PTN to the culture medium, we used substrate-bound PTN because the effects of soluble PTN were transient and low

(Fig. 9). Although PTN induced neurite outgrowth of cerebral neurons (18, 36), this growth factor did not influence the retinoic acid-induced neuritogenesis of Neuro-2A cells (Fig. 10A, B, E, and F). Unexpectedly, when DHA was expressed, retinoic acid-induced neurite extension was remarkably suppressed in Neuro-2A cells on the uncoated plates, and the DHA-expressing cells displayed rounded morphology, like the cells cultured in the absence of retinoic acid (Fig. 10C). In contrast, on the PTN-coated plates, Neuro-2A cells expressing DHA extended neurites in response to retinoic acid, like mock-transfected cells (Fig. 10D, E, and F), indicating that PTN inactivated the DNER activity in Neuro-2A cells.

DISCUSSION

In this study, we demonstrated that PTPζ associates with DNER and regulates the endocytic trafficking of this protein. Recently, it has been recognized that endocytic and exocytic processes play important roles in neurite extension and retraction (41). There are dynamic recycling endosomes in the growth cones, dendrites, and axons regulating the membrane flow in these cellular compartments (5). Our immunohistochemical studies indicated that PTPζ and DNER were partly colocalized at the patchy structures in the dendritic shafts of Purkinje cells (Fig. 3). Further immunoelectron microscopic analysis suggested that these patchy structures correspond to various-sized cytoplasmic vesicles and the plasma membrane. The Purkinje cell plasma membrane facing the Bergmann glial processes often showed PTPζ and DNER immunoreactivities. Previous studies indicated that DNER interacted with coat-associated protein complex AP-1, which mediates polarized targeting of proteins in clathrin-coated transport vesicles (7). It has been suggested that AP-1 recognizes the sorting motifs in the DNER cytoplasmic tail and targets this protein to the somatodendritic compartment through the trans-Golgi network/endosomal system. In addition, it was also proposed that another adaptor protein complex, AP-2, is involved in the clathrin-dependent endocytosis of DNER from the plasma membrane (7). These AP complexes recognize tyrosine-based and dileucine type sorting motifs (6). Both motifs are present in the cytoplasmic region of DNER (Fig. 1), and thus, the DNER-immunoreactive vesicles might correspond to these clathrin-coated vesicles. Classical studies by Altman (1) indicated that there are many coated vesicles in the dendrites of developing Purkinje cells, and PTPζ and DNER might be transported by such vesicles, regulating the dynamic presentation of these proteins on the plasma membrane. At present, immunogold labeling has not been successful because of the low titer of the anti-PTPζ monoclonal antibody. However, further double-immunogold labeling experiments at the electron microscopic level are needed to confirm that both proteins are localized at coated vesicles.

Previously, we reported that inhibition of PTPζ-PTN signaling resulted in the aberrant morphogenesis of cerebellar Purkinje cell dendrites (43). Most of the mature Purkinje cells have only one primary dendrite, which extends toward the pial surface and extensively branches in the molecular layer. However, in the presence of various inhibitors of PTPζ-PTN signaling, Purkinje cells with multiple and disoriented primary dendrites increased in the organotypic slice culture system of the rat cerebellum (43). Forced expression of DdI in the Purkinje cells also induced similar abnormal morphogenesis of Purkinje cell dendrites (Fig. 8). Because of the lack of endocytic sorting signals, this DNER mutant accumulates on the plasma membrane, suggesting that continuous endocytosis of this membrane protein is necessary for the normal morphogenesis of Purkinje cells. Similar phenomena were observed for Neuro-2A transfectants (Fig. 8). Neuro-2A cells expressing DdI extended thick processes, although overexpression of the full-length DNER construct, DHA, resulted in no morphological changes. While DdI was accumulated on the plasma membrane, most of the DHA was internalized and there was little DHA protein on the plasma membrane. Thus, overaccumulation of DNER on the plasma membrane might promote the extension and/or stabilization of odd neurites. Inhibitors of PTPζ-PTN signaling might disturb the endocytosis of DNER in Purkinje cells, leading to the accumulation of DNER on the plasma membrane and to the aberrant morphogenesis of dendrites.

Multiple tyrosine residues in and around the tyrosine-based and dileucine type sorting motifs of the DNER cytoplasmic tail were phosphorylated (Fig. 6). Sodium vanadate inhibited the endocytosis of DNER in COS-7 transfectants (Fig. 7), suggesting that the tyrosine phosphorylation of the DNER cytoplasmic region sterically hinders its association with AP complexes. A similar mechanism was reported for a cell adhesion molecule, L1, by Schaefer et al. (38). They demonstrated that tyrosine phosphorylation at the tyrosine-based sorting motif of the cytoplasmic region of L1 blocked its interaction with the μ2 subunit of AP-2, which led to the inhibition of the internalization of this molecule. Tyrosine-phosphorylated DNER was dephosphorylated by the PTPζ catalytic domain. On the other hand, accumulating evidences demonstrated that PTN induces dimerization of PTPζ, resulting in the inactivation of its phosphatase activity (10, 29). Therefore, we speculate that PTPζ constitutively dephosphorylates DNER, and PTN-induced inactivation of its phosphatase activity leads to the increased tyrosine phosphorylation of DNER and the suppression of its endocytosis. In fact, PTN stimulation of Neuro-2A transfectants increased tyrosine phosphorylation of DNER and suppressed the endocytosis of this protein (Fig. 9).

Recently, Kotani et al. (15) produced transgenic mice expressing a constitutively active form of neuronal src (n-src) kinase selectively in Purkinje cells. The Purkinje cells expressing active n-src showed multiple dendritic shafts extending in nonpolarized directions. This phenotype of Purkinje cells is very similar to that observed when PTPζ-PTN signaling was inhibited (43) or DdI was expressed in Purkinje cells (see above). Active n-src might constantly phosphorylate DNER and induce accumulation of this protein on Purkinje cell surface. Several reports suggested that src kinase is involved in PTN-PTPζ signaling (34, 35). In human endothelial cells, PTN/HARP activated src kinase and focal adhesion kinase through PTPζ, stimulating the migration and tube formation (34). Thus, there is also a possibility that PTN-PTPζ signaling indirectly promotes the tyrosine phosphorylation of DNER through the activation of the src kinase pathway. Further studies are needed to clarify this point.

Recently, it was found that DNER acts as a ligand of Notch receptor and regulates the cell-cell interaction between Pur-

kinje cells and Bergmann glia (8). Bergmann glia strongly express Notch1, which is activated by DNER on Purkinje cells. DNER promoted the process formation of Bergmann glia through Deltex-dependent Notch signaling in vitro. The Bergmann glia in DNER-deficient mice showed retarded formation of radial fibers, reduced expression of GLAST, and ectopic localization in the molecular layer (44). At present, it remains to be determined whether PTPζ signaling affects the Notch pathway in the cerebellar cortex. However, our slice culture experiments indicated that inhibition of PTPζ-PTN signaling led to the reduced expression of GLAST in Bergmann glia (43), suggesting that at least a part of this signaling system is coupled with the DNER-Notch pathway.

It is well known that Notch signaling controls cell fate and various differentiation processes, including neurite outgrowth (3, 4, 37, 39). In this study, we observed that forced expression of DNER in Neuro-2A cells suppressed the retinoic-acid-induced neurite extension (Fig. 10). Because Neuro-2A cells express low levels of Notch1 (9), it might be that DNER activated the Notch1 pathway and inhibited the differentiation of this neuroblastoma by *cis* interaction. However, there is also a possibility that DNER associated with proteins other than Notch and suppressed the differentiation of Neuro-2A cells. PTN reversed this inhibitory activity of DNER and allowed neurite extension induced by retinoic acid, suggesting that endocytosis of DNER is required for the suppression of the differentiation of Neuro-2A cells.

The binding of PTN with phosphacan depends on both the chondroitin sulfate and protein portions of this proteoglycan, and removal of chondroitin sulfate resulted in marked decrease of the binding affinity (22, 25, 26). Phosphacan and PTN are deposited between the Purkinje cell surface and the processes of Bergmann glia, and chondroitinase ABC digestion of cerebellar slices remarkably reduced the PTN content in the tissue (40). In this study, we found that phosphacan did not bind with DdI on COS-7 transfectants, suggesting that phosphacan does not interfere with the PTPζ-DNER or DNER-Notch binding. Instead, phosphacan might serve as a reservoir of PTN secreted by Bergmann glia (25, 27, 43, 45).

Both PTPζ-A and -B isoforms are synthesized as chondroitin sulfate proteoglycans. PTPζ-B lacks a large part of the chondroitin sulfate attachment region (32), suggesting that the affinity of PTPζ-B for PTN is weaker than that of PTPζ-A because of the difference in the number of chondroitin sulfate chains attached to the core proteins. Thus, the strength of PTN-PTPζ signaling could be regulated by the relative expression levels of PTPζ-A and -B. At P6, comparable amounts of PTPζ-A and -B were detected in the cerebellum; however, after that, the expression of PTPζ-A remarkably decreased (Fig. 2A). Before P7, many Purkinje cells have short multiple primary dendrites (40). Thereafter, Purkinje cells vigorously extend dendrites till P20, and most of them have only one primary dendrite after P16 (40). So, strong PTN-PTPζ signaling mediated by PTPζ-A during the early developmental period might allow extension of multiple dendrites by the efficient inhibition of endocytosis of DNER.

Morphological differentiation of Purkinje cells was significantly retarded in the DNER-deficient mice until the second postnatal week; however, this hypoplasia was recovered by the third postnatal week (44). On the other hand, it has been reported that mutant mice deficient in PTPζ showed no gross morphological abnormality in the adult nervous system (11). However, detailed analysis demonstrated that the morphological differentiation of Purkinje cells was retarded in the PTPζ-deficient mice until P8 (unpublished observation). These observations suggest that the loss of DNER and PTPζ can be compensated for by the other signaling molecules. For example, PTPζ deficiency might be compensated for by syndecan 3. Syndecan 3 uses PTN as a ligand, and its function and signal transduction mechanism share many common characteristics with those of PTPζ (2, 13). It will be interesting to analyze the development of Purkinje cells in the mice that are doubly mutant for these genes.

Although it has been suggested that chondroitin sulfate proteoglycans play important roles in the neuron-glia interaction, little is known about the molecular mechanism. This study suggested that PTPζ-PTN signaling regulates Purkinje cell-Bergmann glia interaction by modulating the DNER function. PTPζ-PTN-DNER signaling is a useful system to elucidate the mechanism of chondroitin sulfate proteoglycan-mediated neuron-glia interaction.

ACKNOWLEDGMENTS

We thank Masumi Ichikawa and Kyoko Ajiki for technical assistance and helpful suggestions for immunoelectron microscopic analysis. We also thank Masaharu Noda for allowing us to continue the study of PTPζ.

This work was supported by grants from the Ministry of Education, Science, Sports and Culture of Japan and from the Naito Foundation.

REFERENCES

1. **Altman, J.** 1972. Postnatal development of the cerebellar cortex in the rat. II. Phases in the maturation of Purkinje cells and of the molecular layer. J. Comp. Neurol. **145:**399–463.
2. **Amet, L. E. A., S. E. Lauri, A. Hienola, S. D. Croll, Y. Lu, J. M. Levorse, B. Prabhakaran, T. Taira, H. Rauvala, and T. F. Vogt.** 2001. Enhanced hippocampal long-term potentiation in mice lacking heparin-binding growth-associated molecule. Mol. Cell. Neurosci. **17:**1014–1024.
3. **Artavanis-Tsakonas, S., M. D. Rand, and R. J. Lake.** 1999. Notch signaling: cell fate control and signal integration in development. Science **284:**770–776.
4. **Berezovska, O., P. McLean, R. Knowles, M. Frosh, F. M. Lu, S. E. Lux, and B. T. Hyman.** 1999. Notch1 inhibits neurite outgrowth in postmitotic primary neurons. Neuroscience **93:**433–439.
5. **Blanpied, T. A., D. B. Scott, and M. D. Ehlers.** 2002. Dynamics and regulation of clathrin coats at specialized endocytic zones of dendrites and spines. Neuron **36:**435–449.
6. **Bonifacino, J. S., and L. M. Traub.** 2003. Signals for sorting of transmembrane proteins to endosomes and lysosomes. Annu. Rev. Biochem. **72:**395–447.
7. **Eiraku, M., Y. Hirata, H. Takeshima, T. Hirano, and M. Kengaku.** 2002. Delta/notch-like epidermal growth factor (EGF)-related receptor, a novel EGF-like repeat-containing protein targeted to dendrites of developing and adult central nervous system neurons. J. Biol. Chem. **277:**25400–25407.
8. **Eiraku, M., A. Tohgo, K. Ono, M. Kaneko, K. Fujishima, T. Hirano, and M. Kengaku.** 2005. DNER acts as a neuron-specific Notch ligand during Bergmann glial development. Nat. Neurosci. **8:**873–880.
9. **Franklin, J. L., B. E. Berechid, F. B. Cutting, A. Presente, C. B. Chambers, D. R. Foltz, A. Ferreira, and J. S. Nye.** 1999. Autonomous and non-autonomous regulation of mammalian neurite development by Notch1 and Delta1. Curr. Biol. **9:**1448–1457.
10. **Fukada, M., A. Fujikawa, J. P. Chow, S. Ikematsu, S. Sakuma, and M. Noda.** 2006. Protein tyrosine phosphatase receptor type Z is inactivated by ligand-induced oligomerization. FEBS Lett. **580:**4051–4056.
11. **Harroch, S., M. Palmeri, J. Rosenbluth, A. Custer, M. Okigaki, P. Shrager, M. Blum, J. D. Buxbaum, and J. Schlessinger.** 2000. No obvious abnormality in mice deficient in receptor protein tyrosine phosphatase β. Mol. Cell. Biol. **20:**7706–7715.
12. **Heck, N., A. Klausmeyer, A. Faissner, and J. Garwood.** 2005. Cortical neurons express PSI, a novel isoform of phosphacan/RPTPβ. Cell Tissue Res. **321:**323–333.
13. **Hienola, A., S. Tumova, E. Kulesskiy, and H. Rauvala.** 2006. N-syndecan deficiency impairs neural migration in brain. J. Cell Biol. **174:**569–580.

14. **Kawachi, H., A. Fujikawa, N. Maeda, and M. Noda.** 2001. Identification of GIT1/Cat-1 as a substrate molecule of protein tyrosine phosphatase ζ /β by the yeast substrate-trapping system. Proc. Natl. Acad. Sci. USA **98:**6593–6598.
15. **Kotani, T., N. Morone, S. Yuasa, S. Nada, and M. Okada.** 2007. Constitutive activation of neuronal Src causes aberrant dendritic morphogenesis in mouse cerebellar Purkinje cells. Neurosci. Res. **57:**210–219.
16. **Krueger, N. X., and H. Saito.** 1992. A human transmembrane protein-tyrosine-phosphatase, PTP ζ, is expressed in brain and has an N-terminal receptor domain homologous to carbonic anhydrases. Proc. Natl. Acad. Sci. USA **89:**7417–7421.
17. **Levy, J. B., P. D. Canoll, O. Silvennoinen, G. Barnea, B. Morse, A. M. Honegger, J. T. Huang, L. A. Cannizzaro, S. H. Park, T. Druck, K. Huebner, J. Sap, M. Ehrlich, J. M. Musacchio, and J. Schlessinger.** 1993. The cloning of a receptor-type protein tyrosine phosphatase expressed in the central nervous system. J. Biol. Chem. **268:**10573–10578.
18. **Li, Y. S., P. G. Milner, A. K. Chauhan, M. A. Watson, R. M. Hoffman, C. M. Kodner, J. Milbrandt, and T. F. Deuel.** 1990. Cloning and expression of a developmentally regulated protein that induces mitogenic and neurite outgrowth activity. Science **250:**1690–1694.
19. **Lordkipanidze, T., and A. Dunaevsky.** 2005. Purkinje cell dendrites grow in alignment with Bergmann glia. Glia **51:**229–234.
20. **Maeda, N., F. Matsui, and A. Oohira.** 1992. A chondroitin sulfate proteoglycan that is developmentally regulated in the cerebellar mossy fiber system. Dev. Biol. **151:**564–574.
21. **Maeda, N., H. Hamanaka, T. Shintani, T. Nishiwaki, and M. Noda.** 1994. Multiple receptor-like protein tyrosine phosphatases in the form of chondroitin sulfate proteoglycan. FEBS Lett. **354:**67–70.
22. **Maeda, N., T. Nishiwaki, T. Shintani, H. Hamanaka, and M. Noda.** 1996. 6B4 proteoglycan/phosphacan, an extracellular variant of receptor-like protein-tyrosine phosphatase ζ/RPTPβ, binds pleiotrophin/heparin-binding growth-associated molecule (HB-GAM). J. Biol. Chem. **271:**21446–21452.
23. **Maeda, N., and M. Noda.** 1998. Involvement of receptor-like protein tyrosine phosphatase ζ/RPTPβ and its ligand pleiotrophin/heparin-binding growth-associated molecule (HB-GAM) in neuronal migration. J. Cell Biol. **142:**203–216.
24. **Maeda, N., K. Ichihara-Tanaka, T. Kimura, K. Kadomatsu, T. Muramatsu, and M. Noda.** 1999. A receptor-like protein-tyrosine phosphatase PTPζ/RPTPβ binds a heparin-binding growth factor midkine. Involvement of arginine 78 of midkine in the high affinity binding to PTPζ. J. Biol. Chem. **274:**12474–12479.
25. **Maeda, N., J. He, Y. Yajima, T. Mikami, K. Sugahara, and T. Yabe.** 2003. Heterogeneity of the chondroitin sulfate portion of phosphacan/6B4 proteoglycan regulates its binding affinity for pleiotrophin/heparin binding growth-associated molecule. J. Biol. Chem. **278:**35805–35811.
26. **Maeda, N., N. Fukazawa, and T. Hata.** 2006. The binding of chondroitin sulfate to pleiotrophin/heparin-binding growth-associated molecule is regulated by chain length and oversulfated structures. J. Biol. Chem. **281:**4894–4902.
27. **Matsumoto, K., A. Wanaka, T. Mori, A. Taguchi, N. Ishii, H. Muramatsu, T. Muramatsu, and M. Tohyama.** 1994. Localization of pleiotrophin and midkine in the postnatal developing cerebellum. Neurosci. Lett. **178:**216–220.
28. **Maurel, P., U. Rauch, M. Flad, R. K. Margolis, and R. U. Margolis.** 1994. Phosphacan, a chondroitin sulfate proteoglycan of brain that interacts with neurons and neural cell-adhesion molecules, is an extracellular variant of a receptor-type protein tyrosine phosphatase. Proc. Natl. Acad. Sci. USA **91:**2512–2516.
29. **Meng, K., A. Rodriguez-Pena, T. Dimitrov, W. Chen, M. Yamin, M. Noda, and T. F. Deuel.** 2000. Pleiotrophin signals increased tyrosine phosphorylation of β-catenin through inactivation of the intrinsic catalytic activity of the receptor-type protein tyrosine phosphatase β/ζ. Proc. Natl. Acad. Sci. USA **97:**2603–2608.
30. **Mitsui, K., S. Tsuji, M. Yamazaki, and Y. Nagai.** 1991. Multiple neurite formation in neuroblastoma cell lines by griseolic acid, a potent inhibitor of cyclic nucleotide phosphodiesterases. J. Neurochem. **57:**556–561.
31. **Müller, S., P. Kunkel, K. Lamszus, U. Ulbricht, G. A. Lorente, A. M. Nelson, D. von Schack, D. J. Chin, S. C. Lohr, M. Westphal, and T. Melcher.** 2003. A role for receptor tyrosine phosphatase ζ in glioma cell migration. Oncogene **22:**6661–6668.
32. **Nishiwaki, T., N. Maeda, and M. Noda.** 1998. Characterization and developmental regulation of proteoglycan-type protein tyrosine phosphatase ζ/RPTPβ isoforms. J. Biochem. **123:**458–467.
33. **Pariser, H., P. Perez-Pinera, L. Ezquerra, G. Herradon, and T. F. Deuel.** 2005. Pleiotrophin stimulates tyrosine phosphorylation of β-adducin through inactivation of the transmembrane receptor protein tyrosine phosphatase β/ζ. Biochem. Biophys. Res. Commun. **335:**232–239.
34. **Polykratis, A., P. Katsoris, J. Courty, and E. Papadimitriou.** 2005. Characterization of heparin affin regulatory peptide signaling in human endothelial cells. J. Biol. Chem. **280:**22454–22461.
35. **Qi, M., S. Ikematsu, N. Maeda, K. Ichihara-Tanaka, S. Sakuma, M. Noda, T. Muramatsu, and K. Kadomatsu.** 2001. Haptotactic migration induced by midkine. Involvement of protein-tyrosine phosphatase ζ, mitogen-activated protein kinase, and phosphatidylinositol 3-kinase. J. Biol. Chem. **276:**15868–15875.
36. **Raulo, E., I. Julkunen, J. Merenmies, R. Pihlaskari, and H. Rauvala.** 1992. Secretion and biological activities of heparin-binding growth-associated molecule. Neurite outgrowth-promoting and mitogenic actions of the recombinant and tissue-derived protein. J. Biol. Chem. **267:**11408–11416.
37. **Redmond, L., S. R. Oh, C. Hicks, G. Weinmaster, and A. Ghosh.** 2000. Nuclear Notch1 signaling and the regulation of dendritic development. Nat. Neurosci. **3:**20–40.
38. **Schaefer, A. W., Y. Kamei, H. Kamiguchi, E. V. Wong, I. Rapoport, T. Kirchhausen, C. M. Beach, G. Landreth, S. K. Lemmon, and V. Lemmon.** 2002. L1 endocytosis is controlled by a phosphorylation-dephosphorylation cycle stimulated by outside-in signaling by L1. J. Cell Biol. **157:**1223–1232.
39. **Sestan, N., S. Artavanis-Tsakonas, and P. Rakic.** 1999. Contact-dependent inhibition of cortical neurite growth mediated by notch signaling. Science **286:**741–746.
40. **Shimazaki, Y., I. Nagata, M. Ishii, M. Tanaka, T. Marunouchi, T. Hata, and N. Maeda.** 2005. Developmental change and function of chondroitin sulfate deposited around cerebellar Purkinje cells. J. Neurosci. Res. **82:**172–183.
41. **Shirane, M., and K. I. Nakayama.** 2006. Protrudin induces neurite formation by directional membrane trafficking. Science **314:**818–821.
42. **Snyder, S. E., J. Li, P. E. Schauwecker, T. H. McNeill, and S. R. Salton.** 1996. Comparison of RPTP ζ/β, phosphacan, and trkB mRNA expression in the developing and adult rat nervous system and induction of RPTP ζ/β and phosphacan mRNA following brain injury. Brain Res. Mol. Brain Res. **40:**79–96.
43. **Tanaka, M., N. Maeda, M. Noda, and T. Marunouchi.** 2003. A chondroitin sulfate proteoglycan PTPζ /RPTPβ regulates the morphogenesis of Purkinje cell dendrites in the developing cerebellum. J. Neurosci. **23:**2804–2814.
44. **Tohgo, A., M. Eiraku, T. Miyazaki, E. Miura, S. Y. Kawaguchi, M. Nishi, M. Watanabe, T. Hirano, M. Kengaku, and H. Takeshima.** 2006. Impaired cerebellar functions in mutant mice lacking DNER. Mol. Cell. Neurosci. **31:**326–333.
45. **Wewetzer, K., H. Rauvala, and K. Unsicker.** 1995. Immunocytochemical localization of the heparin-binding growth-associated molecule (HB-GAM) in the developing and adult rat cerebellar cortex. Brain Res. **693:**31–38.
46. **Yamada, K., M. Fukaya, T. Shibata, H. Kurihara, K. Tanaka, Y. Inoue, and M. Watanabe.** 2000. Dynamic transformation of Bergmann glial fibers proceeds in correlation with dendritic outgrowth and synapse formation of cerebellar Purkinje cells. J. Comp. Neurol. **418:**106–120.